

**B. D'ORSI, R. CARCIONE, I. DI SARCINA,  
J. SCIFO, A. VERNA, A. CEMMI**

Nuclear Department  
GAMma irradiation facility Laboratory  
Casaccia Research Centre, Rome - Italy

**A. AMPOLLINI, M.D. ASTORINO,  
G. BAZZANO, C. RONSIVALLE, E. TRINCA**

Nuclear Department  
Particle ACcelerator Laboratory  
Frascati Research Centre, Rome - Italy

**E. MANSI**

Nuclear Department  
Plasma studies and DTT  
Frascati Research Centre, Rome - Italy

# **DOSIMETRIC MEASUREMENTS FOR PRECISE DOSE RATE DISTRIBUTION MAPPING: ENEA CALLIOPE GAMMA IRRADIATION FACILITY AND REX ELECTRON BEAM INTERCALIBRATION**

RT/2025/3/ENEA



ITALIAN NATIONAL AGENCY FOR NEW TECHNOLOGIES,  
ENERGY AND SUSTAINABLE ECONOMIC DEVELOPMENT

B. D'ORSI, R. CARCIONE, I. DI SARCINA,  
J. SCIFO, A. VERNA, A. CEMMI

Nuclear Department  
GAMMA irradiation facility Laboratory  
Casaccia Research Centre, Rome - Italy

A. AMPOLLINI, M.D. ASTORINO,  
G. BAZZANO, C. RONSIVALLE, E. TRINCA

Nuclear Department  
Particle ACcelerators Laboratory  
Frascati Research Centre, Rome - Italy

E. MANSI

Nuclear Department  
Plasma studies and DTT  
Frascati Research Centre, Rome - Italy

# DOSIMETRIC MEASUREMENTS FOR PRECISE DOSE RATE DISTRIBUTION MAPPING: ENEA CALLIOPE GAMMA IRRADIATION FACILITY AND REX ELECTRON BEAM INTERCALIBRATION

RT/2025/3/ENEA



ITALIAN NATIONAL AGENCY FOR NEW TECHNOLOGIES,  
ENERGY AND SUSTAINABLE ECONOMIC DEVELOPMENT

I rapporti tecnici sono scaricabili in formato pdf dal sito web ENEA alla pagina [www.enea.it](http://www.enea.it)

I contenuti tecnico-scientifici dei rapporti tecnici dell'ENEA rispecchiano l'opinione degli autori e non necessariamente quella dell'Agenzia

The technical and scientific contents of these reports express the opinion of the authors but not necessarily the opinion of ENEA.

## DOSIMETRIC MEASUREMENTS FOR PRECISE DOSE RATE DISTRIBUTION MAPPING: ENEA CALLIOPE GAMMA IRRADIATION FACILITY AND REX ELECTRON BEAM INTERCALIBRATION

B. D'Orsi, A. Ampollini, M.D. Astorino, G. Bazzano, R. Carcione, I. Di Sarcina, E. Mansi, C. Ronsivalle, J. Scifo, E. Trinca, A. Verna, A. Cemmi

### **Abstract**

*In the framework of the Italian Space Agency (ASI) Supported Irradiation Facilities (ASIF) program, a campaign of dosimetric measurements was conducted to perform an intercalibration of the Calliope gamma irradiation facility and the REX electron beam. Initially, up-to-date calibration curves for alanine-EPR dosimeters were obtained at the Calliope facility using the absolute Fricke dosimeter. Subsequently, alanine dosimeters were irradiated at multiple positions in the REX chamber by varying distances from the electron source. The resulting dose rate distribution within the chamber was determined. These measurements are essential for optimizing REX irradiation conditions to be used in different applications.*

**Keywords:** *gamma irradiation, electron irradiation, alanine-EPR dosimetry, Fricke dosimetry.*

### **Riassunto**

Nel contesto del programma dell'Agenzia Spaziale Italiana (ASI) ASI Supported Irradiation Facilities (ASIF), è stata condotta una campagna di misure dosimetriche per eseguire l'intercalibrazione tra l'impianto di irraggiamento gamma Calliope e il fascio di elettroni di REX. Inizialmente, sono state ottenute le curve di calibrazione aggiornate per i dosimetri alanina-EPR presso la facility Calliope utilizzando il dosimetro assoluto Fricke. Successivamente, i dosimetri ad alanina sono stati irraggiati in più punti all'interno del bunker di irraggiamento di REX, variando le distanze dalla sorgente di elettroni. È stata così determinata la distribuzione dell'intensità di dose all'interno della camera. Tali misure sono essenziali per ottimizzare le condizioni di irraggiamento all'interno del bunker di REX per applicazioni in diversi campi.

**Parole chiave:** irraggiamento gamma, irraggiamento con elettroni, dosimetria ad alanina, dosimetria Fricke



# INDEX

INTRODUCTION.....	5
1 MATERIALS .....	5
1.1 FRICKE DOSIMETER .....	5
1.2 ALANINE-EPR DOSIMETRY SYSTEM AND EPR THEORY OVERVIEW .....	6
1.2.1 Alanine-EPR dosimeters .....	6
1.2.2 Electron Paramagnetic Resonance spectroscopy .....	7
1.3 RADIOCHROMIC FILM DOSIMETRY FOR X-RAYS AND ELECTRONS.....	10
2 METHODS.....	10
2.1 CALLIOPE FACILITY .....	10
2.2 REX FACILITY .....	11
3 RESULTS AND DISCUSSION: DOSE DISTRIBUTION STUDY .....	12
3.1 ALANINE-EPR CALIBRATION CURVES DETERMINATION AT CALLIOPE FACILITY .....	12
3.2 DOSE RATE DISTRIBUTION MAPPING AT REX .....	13
3.3 RESULTS COMPARISON: ALANINE-EPR AND RADIOCHROMIC FILMS .....	17
3.3.1 Beam homogeneity and dose per pulse .....	19
CONCLUSIONS.....	19
ACKNOWLEDGEMENTS.....	20
REFERENCES .....	20



## Introduction

Dosimetry, primarily in radiology field, is essential for controlling the radiation levels emitted by X-ray machines to ensure the safety of patients and workers, comply with regulatory standards, optimize diagnostic quality, and protect public health. In 1925, the First International Congress of Radiology established the International Commission on Radiological Units (ICRU) to standardize radiation measurement practices in radiology. Dosimetry involves measuring doses of ionizing radiation using dosimeters, which assess energetic particles such as X-rays,  $\gamma$ -rays, neutrons, and charged particles [1]. Radiation dosimeters are classified as absolute if they measure radiation without requiring calibration in a known field. Very often, however, due to the limited dose ranges it is not possible to use absolute dosimetric system and secondary system must be considered.

At the REX facility of the ENEA Frascati Research Center, several dosimetric systems are employed. The output radiation is routinely characterized using radiochromic films (EBT3, HD-V2), a Markus-type ionization chamber, a current transformer and a Faraday collector. These detectors provide information on transverse homogeneity, radiation flux, and machine reproducibility. However, for an accurate dose estimate, comparison with an absolute dosimeter is necessary, particularly for electron modalities characterized by very high dose rates. To this end, dosimetric measurements were performed to establish the electron beam distribution within the REX irradiation bunker. This effort included intercalibration between the Calliope gamma irradiation facility (ENEA Casaccia R.C.) and the REX electron beam irradiation facility (ENEA Frascati R.C.), conducted as part of the Italian Space Agency (ASI) ASIF program [2].

Specifically, alanine-EPR dosimeters were employed due to their suitability for both gamma and electron dosimetry. This report outlines the cross-calibration process, describing how alanine dosimeters were used to assess the radiation dose distribution within the REX irradiation chamber. First, up-to-date calibration curves for the alanine-EPR dosimetry system were obtained using the Fricke dosimetry system at the Calliope facility. Subsequently, alanine dosimeters were irradiated at the REX facility to assess the radiation dose distribution within its irradiation chamber, utilizing the calibration established at Calliope.

This report first introduces Fricke and alanine dosimeters, along with a brief overview of EPR theory. The two facilities involved in the calibration process are then described, followed by the calibration procedure and the methodology used.

## 1 Materials

### 1.1 Fricke dosimeter

The Fricke dosimeter consists of an acidic solution of  $\text{FeSO}_4$ , operating on the principle of radiation-induced oxidation of ferrous ions ( $\text{Fe}^{2+}$ ) to ferric ions ( $\text{Fe}^{3+}$ ) in low pH conditions and in the presence of oxygen. The Fricke dosimeter exhibits a linear response in the 20–200 Gy dose range. Its response remains unaffected by radiation energy in the range of 0.1–16 MeV and by dose rates ranging from 0.2 to  $1 \times 10^7$  Gy/s. During irradiation, temperature variations between 1 °C and 60 °C have negligible effects on the dosimeter's response. The limited absorbed dose range (20–200 Gy) is due to inaccurate measurements below 20 Gy and oxygen consumption at higher absorbed doses. The Fricke dosimeter is considered an absolute dosimeter because it directly provides the absorbed dose by measuring the change in absorbance, also known as Optical Density (OD), of the solution due to irradiation. The absorbance measurement is often used to determine the concentration of a substance in a solution

based on the Beer-Lambert Law that describes the relationship between the absorption of light by a substance and the properties of that substance [3]. The absorbance is defined as:

$$A = \text{Log}_{10}(I_0/I) \quad (1)$$

where  $I_0$  is the incident light intensity and  $I$  is the intensity of light transmitted after traversing the sample. To quantitatively analyze the concentration of  $\text{Fe}^{3+}$  produced by irradiation in the Fricke dosimeter, the absorbance of the solution at 304 nm is measured using a UV-Vis spectrophotometer. Figure 1 illustrates an example setup of this measurement.

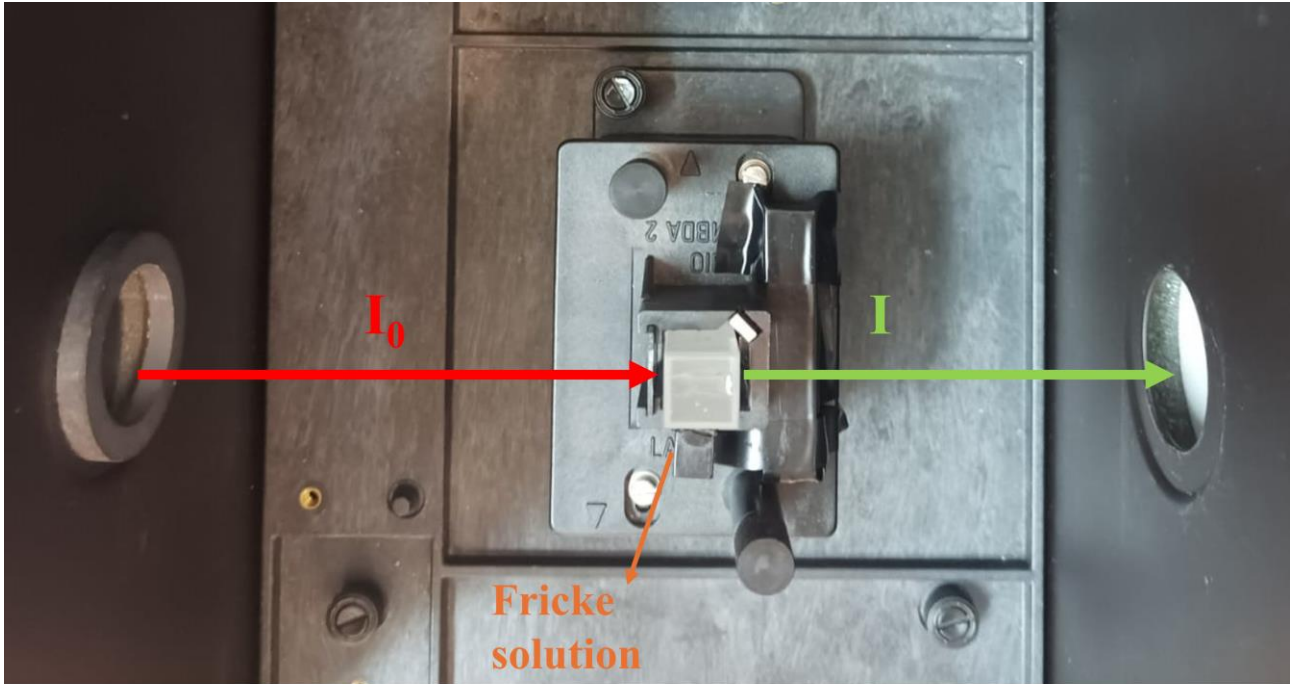


Figure 1. Example setup of Fricke dosimeter measurement using a UV-Vis spectrophotometer.  $I_0$  represents incident light intensity (red arrow) and  $I$  is transmitted light intensity (green arrow) after passing through the cuvette containing Fricke solution.

The relationship between the absorbed dose (in Gy) and the optical density (OD) for the Fricke dosimeter is given by:

$$D = \Delta(OD) \cdot \epsilon \cdot G(\text{Fe}^{3+}) \cdot \rho \cdot l \quad (2)$$

where  $\Delta(OD)$  is the change in the solution's optical density due to irradiation,  $\epsilon$  is the molar extinction coefficient of ferric ions at 304 nm ( $\epsilon(\text{Fe}^{3+}) \approx 220 \text{ m}^2/\text{mol}$ ),  $G(\text{Fe}^{3+})$  is the number of ferric ions produced per unit of absorbed energy ( $G(\text{Fe}^{3+}) = (1.61 \pm 0.03) \times 10^{-6} \text{ mol/J}$  for a  $^{60}\text{Co}$  source),  $\rho$  is the density of the irradiated solution ( $\rho = 1024 \text{ kg/m}^3$ ), and  $l$  is the optical path length ( $l = 1 \text{ cm}$ ).

## 1.2 Alanine-EPR dosimetry system and EPR theory overview

### 1.2.1 Alanine-EPR dosimeters

The alanine-EPR dosimetry system is suitable for gamma rays, electrons, and X-rays, offering several advantages: it features high signal stability, a wide absorbed dose range (20 Gy – 200 kGy), and is nearly independent of dose rate and energy. It is also relatively insensitive to environmental factors such as light, humidity, and temperature. The alanine-EPR dosimetry system is considered one of the most effective dosimetric techniques and is based on detecting stable free radicals induced by ionizing radiation in the crystalline L- $\alpha$ -alanine amino acid through Electron Paramagnetic Resonance (EPR)

spectroscopy [4]. When alanine amino acid ( $\text{CH}_3\text{-CHNH}_2\text{-COOH}$ ) is irradiated, it forms a stable  $\text{CH}_3\text{-}\dot{\text{C}}\text{H-COOH}$  free radical at room temperature. The number of induced free radicals is proportional to the absorbed dose.

### 1.2.2 Electron Paramagnetic Resonance spectroscopy

EPR spectroscopy, also known as Electron Spin Resonance spectroscopy, provides insights into both the type and quantity of free radicals present in samples, making it a valuable tool for studying the characteristics and behavior of these radical species [5]. This spectroscopy is used to investigate the structure and behavior of radicals in materials that contain unpaired electrons. Electrons, being charged particles with mass and spin  $s = 1/2$ , have intrinsic magnetic properties characterized by their spin quantum number  $m_s$  which can be  $m_s = +1/2$  (spin-up) or  $m_s = -1/2$  (spin-down). The rotation of the electron (its spin) generates a magnetic moment. In the presence of an external magnetic field  $B_0$ , the energy levels associated with the two spin states of the electron, which are normally degenerate (having the same energy), become separated due to the interaction between the external magnetic field and the magnetic moment of the electron. This phenomenon is illustrated in Figure 2.

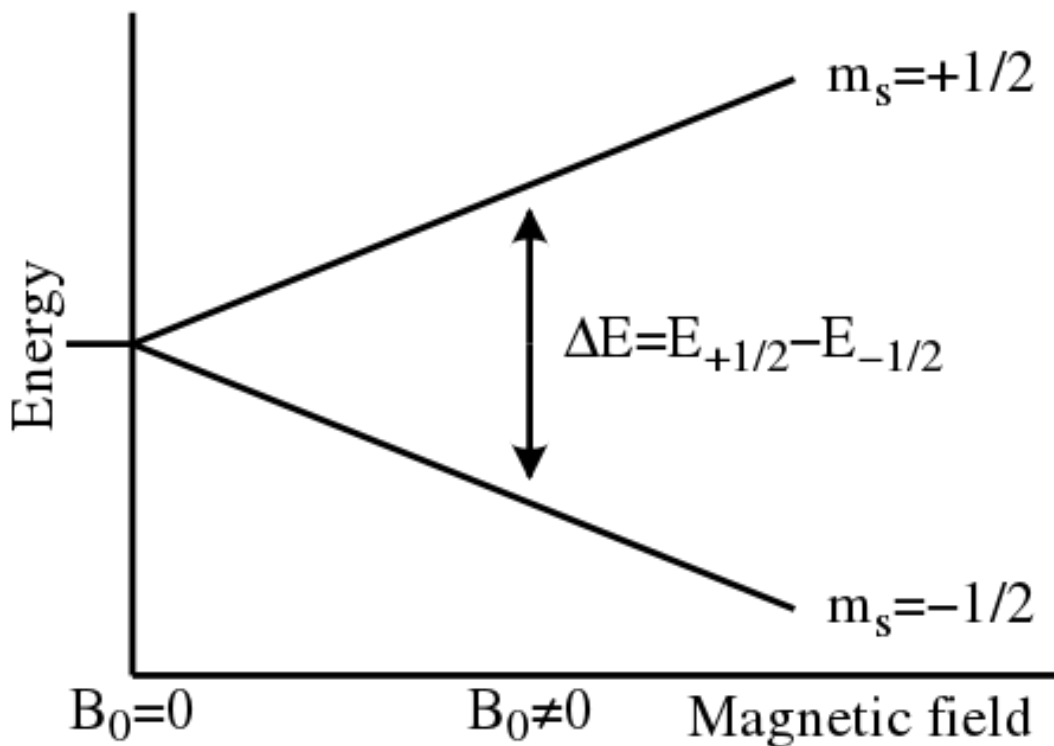


Figure 2. Splitting of the electron spin energy levels due to the interaction of the external magnetic field  $B_0$  with the electron magnetic moment, as a function of the applied magnetic field  $B_0$ .

The energy difference associated to the two spin levels is defined as:

$$\Delta E = g_E \mu_B B_0 \quad (3)$$

where  $B_0$  is the applied magnetic field,  $\mu_B$  is a constant named Bohr magneton ( $\mu_B = 9.27 \cdot 10^{-21}$  erg/gauss) and  $g_E$  is a dimensionless factor, called  $g$ -factor. The  $g$ -factor characterizes the ratio between the magnetic moment and the angular momentum of a particle and for a free electron it is equal to  $g_E = 2.0023$ . Since both  $g_E$  and  $\mu_B$  are constant, the energy splitting is proportional to the magnetic field strength. When the electron is exposed to an electromagnetic field characterized by a frequency  $\nu$  that meets the resonance condition:

$$h\nu = g_E \mu_B B_0 = E_{+1/2} - E_{-1/2} \quad (4)$$

the transition between the two energy levels is allowed, enabling the unpaired electron to absorb a photon with energy  $h\nu$  and move between these states [6]. Equation 4 represents the core equation in EPR spectroscopy. In this technique, the frequency  $\nu$  is determined by the dimensions of the resonant cavity of the spectrometer, while the applied magnetic field  $B_0$  is varied. This is crucial for tuning the resonance of response to the magnetic field. The  $g$ -factor depends on the nature of the half-filled orbital, meaning the type of atomic or molecular orbitals containing unpaired electrons. In some cases, the  $g$ -factor may also depend on the orientation of the orbital relative to the applied magnetic field. For example, the orientation of p or d orbitals in a crystal field can affect the value of the  $g$ -factor. An EPR spectrometer consists of a cavity situated within an electromagnet enabling continuous variation of the applied magnetic field. It includes a microwave source that emits microwave radiation into the cavity, a sample cell placed inside the cavity to interact with both the microwaves and the varying magnetic field and a detector capable of measuring the intensity of the radiation absorption. Solid-state diodes are often used as detectors because they are sensitive to microwave energy, detecting absorption lines when the energy level separation matches the microwave frequency. Most external components, such as the source and detector, are housed within a microwave bridge control [7]. Figure 3 illustrates a schematic diagram of an EPR spectrometer.

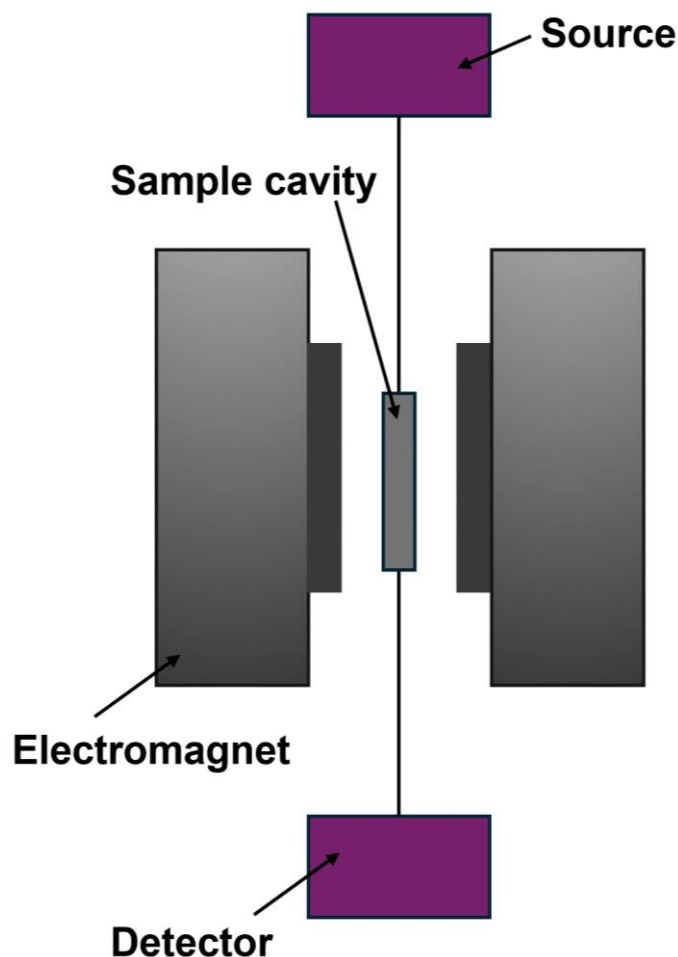


Figure 3. Scheme of a typical EPR spectrometer. Adapted from [7].

In alanine-EPR dosimeter measurements, the alanine samples are placed into a vertical quartz tube and then inserted into the EPR microwave cavity where the magnetic field can be adjusted (quartz tubes are preferred in EPR spectroscopy because they are highly resistant to the formation of free radicals compared to other types of glass or insulating materials). When the external magnetic field of the

spectrometer matches the energy difference between the split levels, absorption occurs and a signal is detected. EPR spectra are recorded as the first derivative of this absorption signal. This method enhances the intensity of the detectable signal, making it easier to observe and analyze EPR spectra even under low absorption conditions.

An example of an alanine-EPR spectrum after irradiation exposure is shown in Figure 4, highlighting the maximum peak-to-peak height ( $h_{pp}$ ) that is a commonly used parameter in EPR spectroscopy.

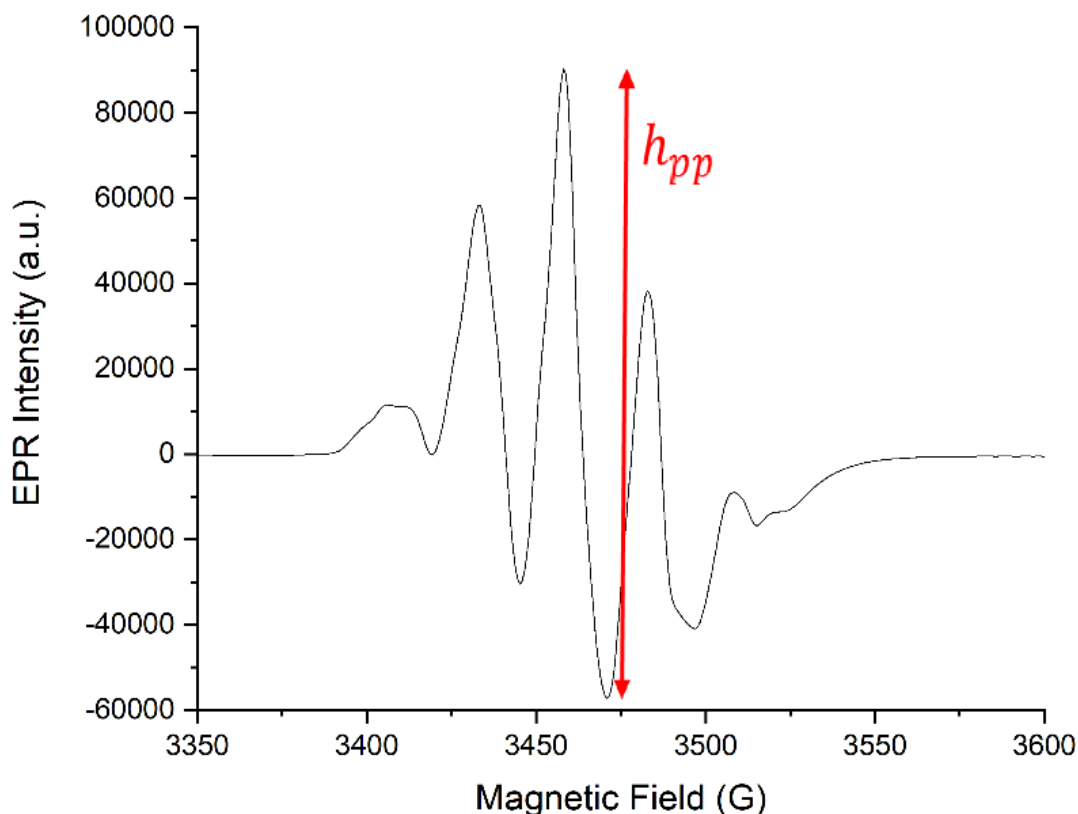


Figure 4. EPR spectrum of an alanine pellet after irradiation. The maximum peak-to-peak height ( $h_{pp}$ ) is shown.

From Figure 4, it is evident that the alanine spectrum after irradiation is characterized by five main peaks. The area of the EPR signal (the double integral of the spectrum since the spectrum is the derivative of the absorption signal) and the  $h_{pp}$  parameter are directly proportional to the number of radiation-induced radicals, which correlates with the absorbed dose.

The results presented in this report were obtained with alanine pellets from Aerial [8]. These dosimeters consist of pressed alanine powder pellets with wax as binding material (approximately 5%). The pellets, shown in Figure 5a, are approximately 2.3 mm thick and have a diameter of about 4.0 mm.

Alanine-EPR analysis was conducted using a Bruker e-scan EPR spectrometer (Figure 5b), operating at 9.4 GHz in the X-band with a microwave power of 0.14 mW and a magnetic field range of 3350–3650 G.

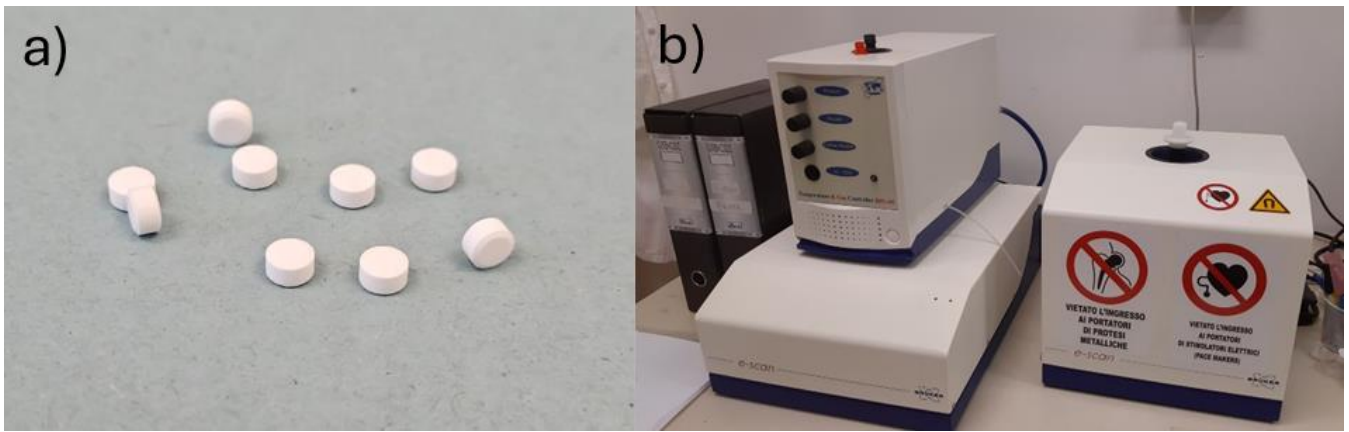


Figure 5. Picture of a) alanine pellets from Aerial and b) Bruker e-scan EPR spectrometer.

An optimization of the measurement procedure was performed prior to those described in this study [9].

### 1.3 Radiochromic film dosimetry for x-rays and electrons

Radiochromic film dosimeters allow quantitative measurement of absorbed dose of photons and charged particles. They are routinely employed in clinical applications, especially for dose verification in external beam radiotherapy, thanks to their near tissue-equivalence, high spatial resolution and ease of use. In fact, self-developing films do not require specific handling and acquisition can be performed with transmission densitometers, spectrophotometers but also commercially available professional photo scanners.

In the NUC-TECFIS-ACP laboratory, Ashland [10] films are employed and acquired with an EPSON Expression 11000XL flatbed scanner. These films are made up of a thin, active layer and a substrate layer. The active layer can either be coated on a substrate or sandwiched between two substrate layers. Different types of radiochromic films cover different dose ranges and dose sensitivity and, additionally, various configurations of active layer and substrate geometry allow selection of the best film type for each radiation source. The HD-V2 type films are characterized by high saturation dose (1 kGy) and a single layer of substrate and are suitable for high dose rate electron beam. For X-rays, whose dose rate is significantly lower, EBT3 films, which saturate at 20 Gy, are employed.

The recommended calibration procedure for the use of HD-V2 films in high accuracy dosimetric applications, such as radiotherapy, is described in [10] and requires exposure of samples of films from each batch to at least 6-8 dose levels in the 0-1000 Gy range at a reference radiation source.

However, even in the absence of a specific calibration, radiochromic films are often employed to obtain relative dose information and retrieve dose homogeneity maps. To this end, an absolute calibration curve for radiochromic films reported in [16] is used. The curve is expected to give dose values with accuracy within  $\pm 10\%$ .

## 2 Methods

### 2.1 Calliope facility

The Calliope facility, located at the ENEA Casaccia Research Center, is a pool-type gamma irradiation facility equipped with a  $^{60}\text{Co}$  radioisotope source array (mean energy 1.25 MeV) [11]. The irradiation cell has dimensions of  $7.0 \times 6.0 \times 3.9 \text{ m}^3$  and houses a source rack with 25 source rods in a planar geometry (Figure 6).



Figure 6. a) Calliope source rack in the pool and b) source rack within the irradiation cell (picture acquired by remote camera).

The maximum licensed activity for the Calliope plant is  $3.7 \cdot 10^{15}$  Bq (100 kCi) and, positioning a sample at different distances with respect to the source rack within the irradiation cell, it is possible to perform irradiation at different dose rate values; in particular, the maximum available dose rate is approximately 5 kGy/h (January 2025).

The steel platform, shown in Figure 6b, is installed to enable samples positioning close to the irradiation source and to perform irradiation at high dose rate values. At Calliope facility it is also possible to perform irradiation tests in different environmental conditions. A dosimetric and characterization laboratory is also available at the facility. The dosimetric systems used include the Fricke solution [12], alanine-EPR, Red Perspex, TLD, RADFET and online dose rate sensors, suitable for different dose ranges. The Fricke solution, which is used as absolute dosimeter, serves as the reference for calibrating the other systems. The process of calibration involves irradiating relative dosimeters at the same locations where dose rates are measured using the Fricke system.

## 2.2 REX facility

The REX (Removable Electron to X-ray) facility [13], [14], located at the ENEA Frascati Research Center, employs a 5 MeV electron linear accelerator (linac) to produce a pulsed electron beam. The REX linac consists of an S-band, standing-wave accelerating structure and a radiofrequency source based on a 2 MW magnetron powered by a Pulse Forming Network (PFN). The electrons are generated in the e-gun by a cathode powered by a second PFN. The electron beam energy and peak current can be varied actively, within the range allowed by the load line, through variation of the power provided to the cathode and magnetron.

The electron beam is extracted in air through a Titanium window and can be converted into X-rays by positioning a tungsten conversion target immediately after the linac extraction window.

The REX extraction line is not equipped with optics elements to focus or shape the electron beam in the transverse plane, therefore the beam is characterized by a certain angular divergence, that is further increased by the scattering with the air molecules as the beam travels downstream the extraction window.

The REX accelerator is placed in a bunker hosted in the ENEA Frascati particle accelerators building; irradiations are carried out inside a lead-shielded irradiation chamber of  $40 \times 40 \times 80$  cm<sup>3</sup> size. A schematic of the REX plant is depicted in Figure 7.

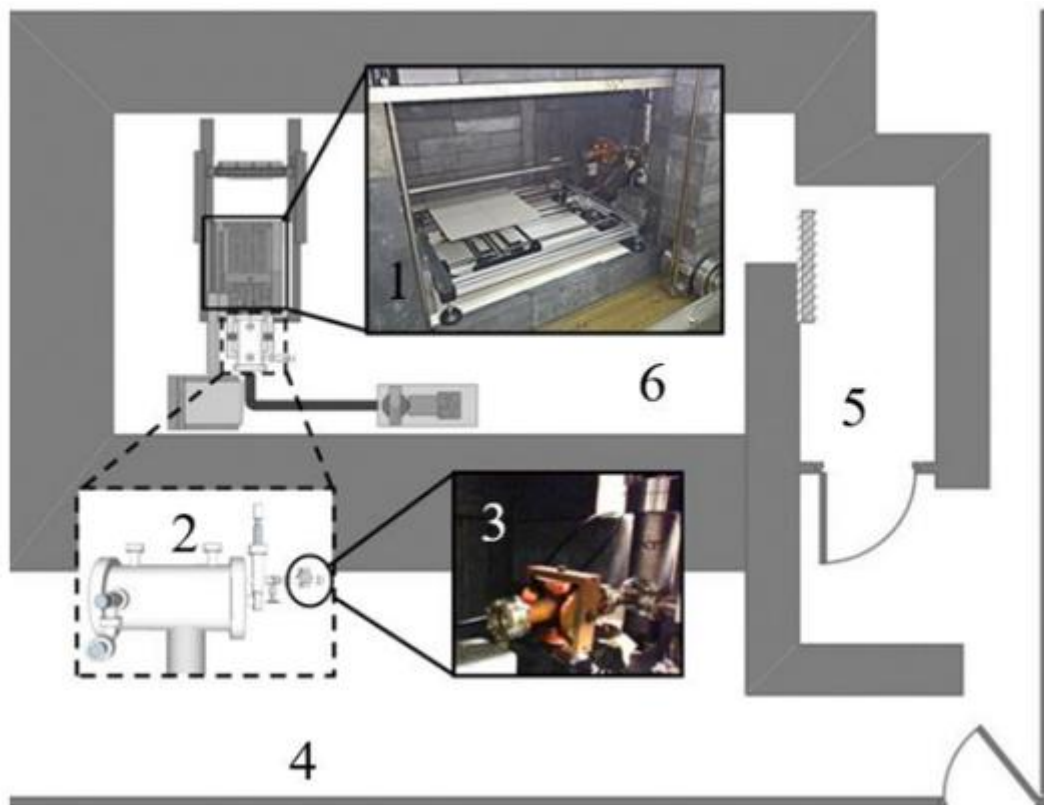


Figure 7. Scheme of the REX facility. (1)Irradiation chamber, (2) vacuum vessel containing the linac, (3) linac extraction point, (4) control room and (5) bunker access are highlighted [13].

The maximum pulse repetition frequency of the linac is 20 Hz, with a typical pulse width of 3.4  $\mu$ s. The beam maximum peak current is 150 mA.

The REX facility routinely uses HD-V2 radiochromic films [10] for electron beam diagnostics and dosimetry, as well as the PPC05 Markus-type ionization chamber [15], primarily used for X-ray measurements. Given the high dose rates typical of electron beams in the REX irradiation chamber, radiochromic films are more suitable for dose measurement. However, these films are not absolute dosimeters and require calibration.

### 3 Results and discussion: dose distribution study

#### 3.1 Alanine-EPR calibration curves determination at Calliope facility

The calibration process of secondary dosimeters, such as alanine-EPR, involves several steps:

- **Measurements of absorbed dose rate:** the absorbed dose rate at specific positions in the irradiation cells is measured using the Fricke absolute method;
- **Alanine irradiation:** alanine pellets are then irradiated in the same positions within the irradiation cell where the dose rate was measured using Fricke dosimetry;
- **Calculation of absorbed dose:** the absorbed dose is determined by considering the dose rate measured by the Fricke method (corrected for the decay of the  $^{60}\text{Co}$  source which accounts for the decrease in radioactivity of the  $^{60}\text{Co}$  source over time) and the irradiation time of the alanine pellets;

• **Calibration curve determination:** after irradiation, each alanine pellet is analyzed to investigate the quantity of free radicals induced by ionizing radiation. These measurements are used to establish a calibration curve correlating the quantity of free radicals with the absorbed dose.

To obtain the calibration curves used for the dose rate distribution mapping within the REX irradiation bunker, alanine pellets were irradiated at specific positions within the Calliope irradiation cell, with dose rates determined using Fricke dosimetry. Absorbed doses were calculated based on irradiation times and subsequently correlated with free radical formation in alanine dosimeters, measured by EPR, to establish calibration curves. Two distinct calibration curves were developed, one for low dose and one for high-dose range (Figures 8a and 8b), reflecting different EPR parameters.

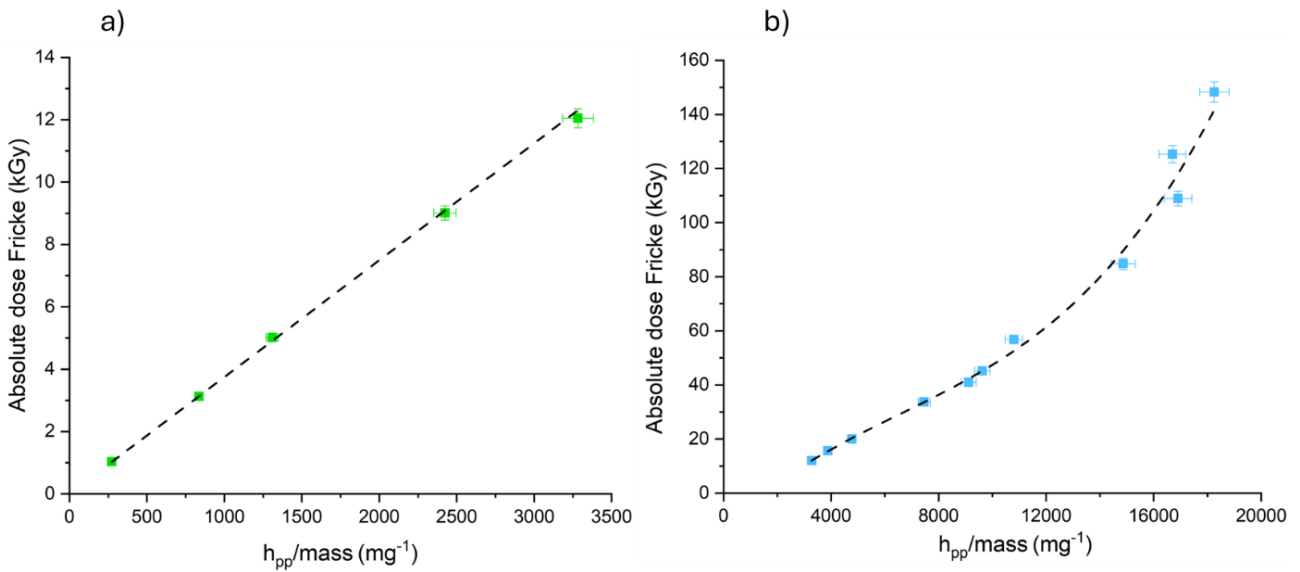


Figure 8. Alanine-EPR a) low dose range and b) high dose range calibration curves.

The calibration curve for alanine-EPR dosimetry indicates the total absorbed dose ( $D^{total}$ ) dependence on the amplitude of the maximum peak-to-peak height of the EPR spectrum normalized to the alanine pellet mass  $\frac{h_{pp}}{mass}$ . The low-dose range calibration curve corresponds to absorbed dose values below 12 kGy. The interpolation of experimental data presented in the calibration curve obtained for the low-dose range gives:

$$D^{total} [Gy] = 0.00375 \frac{h_{pp}}{mass} \quad (1)$$

For the high-dose range calibration curve (above 12 kGy), the experimental data yield:

$$D^{total} = -12.4 + 0.0093 \left( \frac{h_{pp}}{mass} \right) - 6.73 \cdot 10^{-7} \left( \frac{h_{pp}}{mass} \right)^2 + 3.43 \cdot 10^{-11} \left( \frac{h_{pp}}{mass} \right)^3 \quad (2)$$

These calibration curves allow for accurate determination of absorbed doses within alanine pellets following irradiation, based on EPR measurements of  $\frac{h_{pp}}{mass}$  values.

### 3.2 Dose rate distribution mapping at REX

In the absence of a dedicated absolute dosimetric system for the REX electron beam, the alanine dosimetry system, calibrated at the Calliope facility with <sup>60</sup>Co photons, serves as an absolute dosimeter. Alanine dosimeters response is not significantly affected by the type of radiation, whether photons or

electrons. The response in electron beams is only 1-2% lower than that in  $^{60}\text{Co}$ . Consequently, alanine pellets were irradiated with the REX 5 MeV electrons, and dose values were obtained using alanine-EPR calibration curves from the Calliope facility. To investigate the dose distribution within the REX irradiation chamber, the dosimeters were positioned at different points on a 20 x 20 cm<sup>2</sup> sample holder, as shown as an example in Figure 9 for three pellets placed on the central row (9th row).

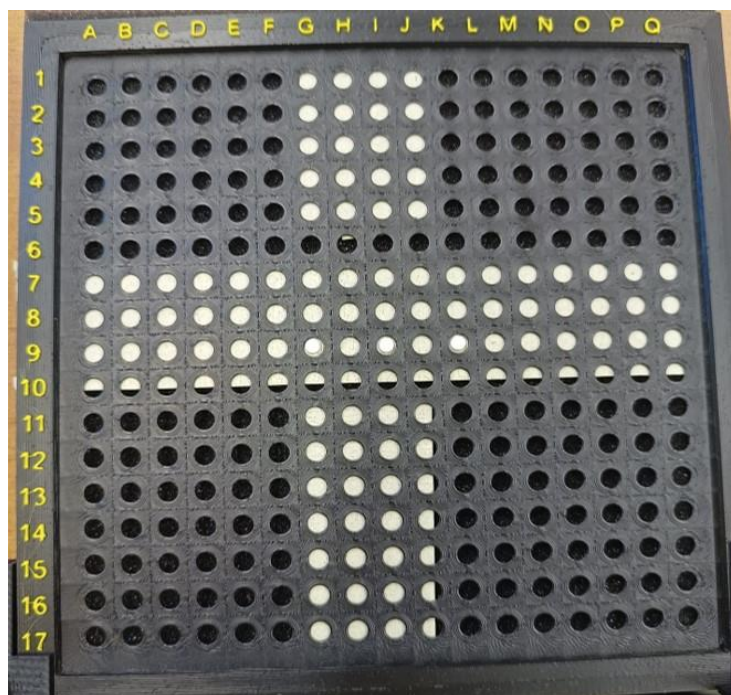


Figure 9. Picture of three alanine pellets positioned on the central row in the position G9, I9 and K9 of the 20 x 20 cm<sup>2</sup> sample holder.

The distance between adjacent holes of the holder is 1 cm. The alanine pellets were identified according to their position on the sample holder (i.e. the letter of the column and the number of the row from Figure 9). Three irradiation tests were performed with the sample holder positioned at 20 cm, 30 cm, and 40 cm from the linac exit window, transversely with respect to the beam propagation. The hole I9 of the sample holder was centered with respect to the exit of the linac. For all irradiation tests, the Pulse Repetition Frequency (PRF) was set at 15 Hz. The irradiation conditions (distance of the sample holder from the linac exit and irradiation time) are summarized in Table 1.

Irradiation tests	Distance (cm)	Time (s)
1	20	15.2
2	30	60.2
3	40	90.1

Table 1. Summary of alanine irradiation conditions at REX facility with a 5 MeV electron beam.

Each irradiated alanine pellet was measured three times with the EPR Bruker e-scan. Between repeated measurements, the dosimeter was rotated around its longitudinal axis. The reading reproducibility of the dosimeter for a given irradiation condition was about 1-2%. The mean value of the three measurements of the maximum peak-to-peak amplitude of the EPR spectrum normalized to the sample mass was considered. The mean value of  $\frac{h_{pp}}{mass}$  obtained for each irradiated alanine pellet was reported in the alanine calibration curve made at the Calliope facility to obtain an absorbed dose value. Specifically, for each dosimeter, a dose value was obtained with the low dose range calibration curve

(Figure 8a), substituting  $\frac{h_{pp}}{mass}$  in Equation 1. The results obtained are summarized in Table 2 at a distance of 20 cm, Table 3 at a distance of 30 cm and Table 4 at a distance of 40 cm.

Alanine position	Mean $h_{pp}/mass$ ( $mg^{-1}$ )	Absorbed dose (Gy)	Dose rate (Gy/s)
F9	147.7	554	36.5
G9	405.0	1519	100.2
H9	938.0	3517	232.0
I6	357.7	1341	88.5
I7	815.9	3060	201.8
I8	1367.1	5127	338.2
I9	1630.2	6113	403.2
I10	1248.7	4683	308.9
I11	692.8	2598	171.4
I12	281.7	1057	69.7
J9	1911.8	7169	472.9
K9	1511.0	5666	373.8
L9	755.7	2834	186.9
M9	306.0	1147	75.7
N9	82.7	310	20.5

Table 2. Summary of the results obtained after irradiation with a 5 MeV electron beam of alanine pellets positioned at different points on the sample holder (identified by the letter of the column and the number of the row from Figure 9a) at a distance of 20 cm from the linac exit. The uncertainty of the mean  $h_{pp}/mass$  value is  $\pm 1\%$  and the error on the absorbed dose and dose rate due to calibration uncertainties is 5%.

Alanine position	Mean $h_{pp}/\text{mass}$ ( $\text{mg}^{-1}$ )	Absorbed dose (Gy)	Dose rate (Gy/s)
E9	504.6	1892	31.4
G9	1382.8	5185	86.1
I5	734.3	2753	45.7
I7	1728.9	6483	107.7
I9	2395.5	8983	149.2
I11	1717.3	6440	107.0
I13	730.2	2738	45.5
K9	2177.6	8166	135.6
M9	1092.1	4095	68.0
O9	353.0	1324	22.0

Table 3. Summary of the results obtained after irradiation with a 5 MeV electron beam of alanine pellets positioned at different points on the sample holder (identified by the letter of the column and the number of the row from Figure 9a) at a distance of 30 cm from the linac exit. The uncertainty of the mean  $h_{pp}/\text{mass}$  value is  $\pm 1\%$  and the error on the absorbed dose and dose rate due to calibration uncertainties is 5%.

Alanine position	Mean $h_{pp}/\text{mass}$ ( $\text{mg}^{-1}$ )	Absorbed dose (Gy)	Dose rate (Gy/s)
E9	869.7	3261	36.2
G9	1661.2	6229	69.1
I5	1114.9	4181	46.4
I7	1903.4	7138	79.2
I9	2402.5	9009	100.0
I11	2005.1	7519	83.4
I13	1207.3	4527	50.2
K9	2325.5	8721	96.8
M9	1561.2	5855	65.0
P9	516.6	1937	21.5

Table 4. Summary of the results obtained after irradiation with a 5 MeV electron beam of alanine pellets positioned at different points on the sample holder (identified by the letter of the column and the number of the row from Figure 9a) at 40 cm from the linac exit. The uncertainty of the mean  $h_{pp}/\text{mass}$  value is  $\pm 1\%$  and the error on the absorbed dose and dose rate due to calibration uncertainties is 5%.

The maximum dose rate was found at 20 cm from the linac exit, specifically in hole J9, which is at 1 cm from the center position I9, aligned with respect to the exit point. This displacement is due to a centroid horizontal angle of the beam exiting from the linac. In Figure 10a, the dose rate variation with the distance from the linac exit in position I9 is plotted. From Figure 10a it is evident that the dose rate

decreased significantly with the distance from the linac exit, following approximately a  $1/r^2$  law as a function of the distance  $r$  from the linac exit window. This is consistent with a representation of the electron beam as emitted from a “point source” (the exit window); as the beam diverges from the source, the electron fluence decreases

Considering the absorbed dose values corresponding to alanine pellets irradiated on the 9th row of the sample holder, the transverse distributions of the dose at fixed distances from the linac exit were obtained. Specifically, the transverse dose rate beam profiles obtained for the irradiation performed at 20 cm, 30 cm and 40 cm are shown in Figure 10b. For all the studied distances from the linac exit, the transverse profiles exhibit a similar symmetric decrease in dose rate away from the central position. These profiles provide the spatial distribution of the dose rate within the irradiation chamber, which is essential for dosimetric studies and ensuring uniform irradiation of samples.

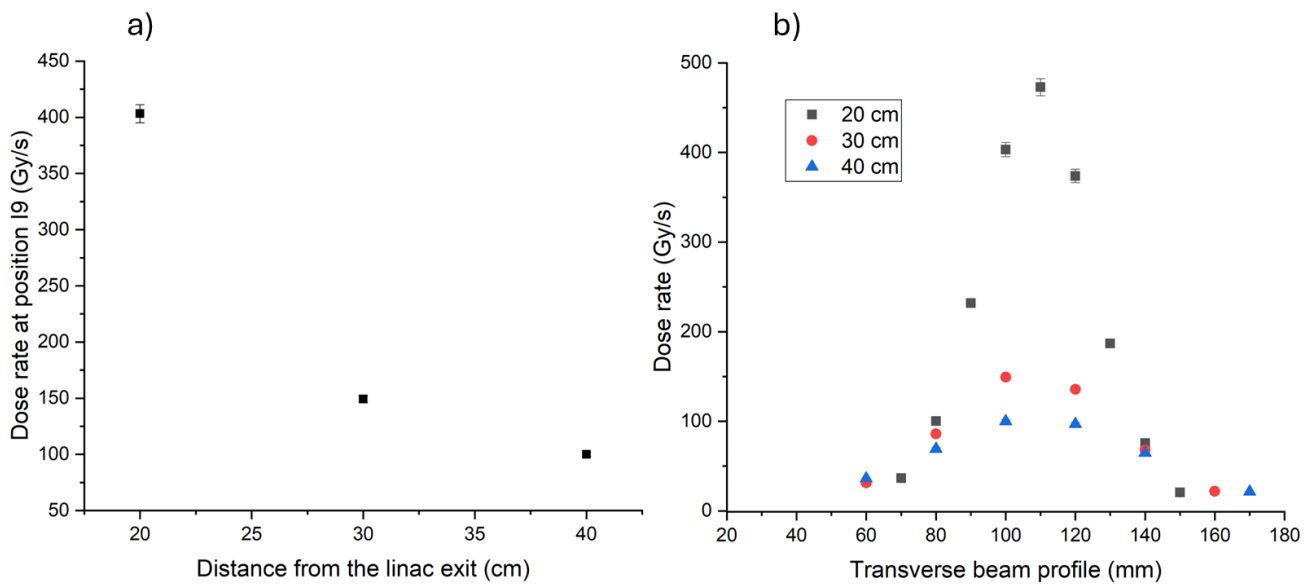


Figure 10. a) Dose rate variation with distance from the linac exit in the central position of the sample holder and b) transverse beam profiles obtained with alanine dosimetry system after irradiation at 20 cm, 30 cm and 40 cm from the linac exit.

### 3.3 Results comparison: alanine-EPR and radiochromic films

To further validate the alanine dosimetry system,  $20 \times 20$  cm<sup>2</sup> HD-V2 Gafchromic films were used to assess the beam homogeneity. The films were irradiated at the same accelerator setting used for alanine irradiations, but for a shorter duration to avoid saturation of the HD-V2 films (maximum dose  $\approx$  1 kGy). The films were positioned perpendicularly to the electron beam propagation between two slabs of water-equivalent solid phantom by Scanditronix (density of 1.035 g/cm<sup>3</sup>) at distances of 30 cm and 40 cm from the linac exit. After irradiation, the radiochromic films were scanned using an Epson flatbed Expression 11000XL scanner. An example of the HD-V2 image after irradiation at 30 cm from the linac exit is shown in Figure 11.

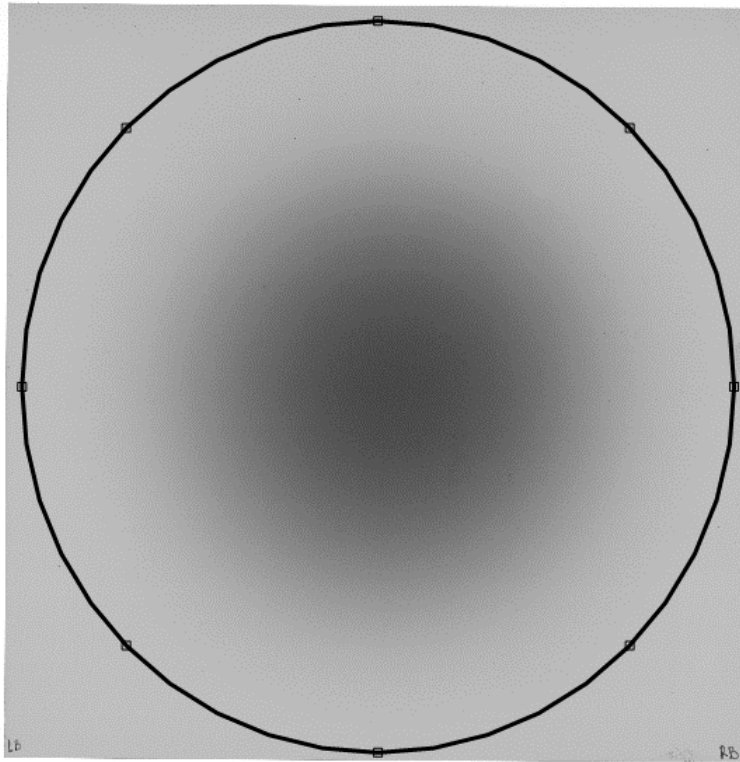


Figure 11. HD-V2 Gafchromic film after irradiation at 30 cm from the linac exit and detail of the Region Of Interest (ROI) identified for the analysis. The image was acquired using an Epson flatbed Expression 11000XL scanner.

The corresponding absorbed dose was calculated using the absolute calibration curve for radiochromic films reported in [16].

The transverse beam profiles of the absorbed dose, normalized to the maximum value, obtained with Gafchromic systems, reported in Figure 12, were found to be in good agreement with the results from the alanine dosimetry system on a very broad range of doses: from a maximum dose value  $\approx 1$  kGy down to less than 100 Gy. This demonstrated that the also in absence of a specific calibration procedure the gaf analysis approach described in [16] can be employed to measure the electron beam transverse profile with gafchromic films obtaining accurate and high resolution normalized dose maps.

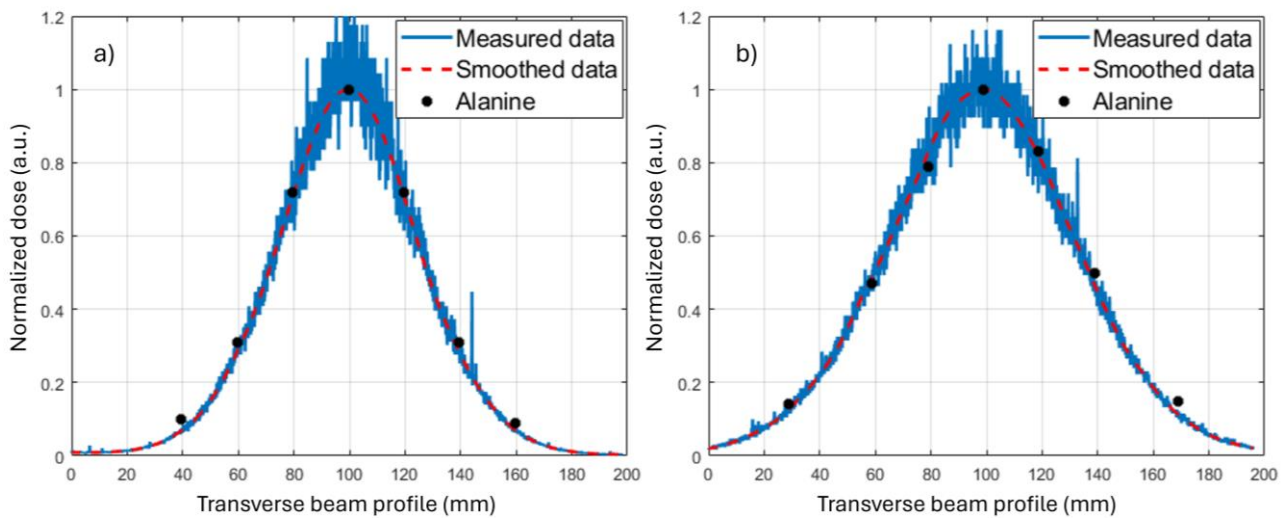


Figure 12. Transverse beam profiles normalized to the maximum dose value, obtained with HD-V2 Gafchromic films (Measured data and Smoothed data) and with the alanine dosimetry system for irradiations performed at (a) 30 cm and (b) 40 cm from the linac exit.

Notably, both dosimetric systems reveal similar dose distributions, validating the calibration methods employed in both the Calliope and REX facilities.

### 3.3.1 Beam homogeneity and dose per pulse

The beam homogeneity was assessed using the Full Width at Half Maximum (FWHM) and Full Width at 80% Maximum (FW80%M) parameters. The latter quantifies the width of the dose profile at 80% of the maximum dose, corresponding to the diameter of a circular spot with  $\pm 10\%$  homogeneity. The values of FWHM and FW80%M for irradiations performed at 30 cm and 40 cm from the linac exit are summarized in Table 5.

	d = 30 cm	d = 40 cm
FWHM (mm)	57.1	77.3
FW80%M (mm)	31.9	42.5
Maximum dose (Gy)	964	491
Maximum dose rate (Gy/s)	192.8	98.2
Mean dose (Gy)	896.9	456.7
Mean dose rate (Gy/s)	179.4	91.3

Table 5. Parameters corresponding to the transverse beam profile for irradiations performed at distances of 30 cm and 40 cm from the REX linac exit as measured by HD-V2 films.

At both distances, the results indicate a beam profile characterized by approximately  $\pm 10\%$  homogeneity within a circular area of about 32 mm in diameter at 30 cm and 43 mm at 40 cm.

In addition, the dose per pulse was calculated for both the alanine dosimeters and the radiochromic films. The values of dose per pulse were 10.5 Gy/pulse at 30 cm and 6.6 Gy/pulse at 40 cm for the alanine dosimeters, and 12 Gy/pulse and 6.1 Gy/pulse for the HD-V2 films. These results demonstrate that both dosimetric systems are consistent in measuring the dose delivered by the electron beam.

## Conclusions

The dosimetric intercalibration of the Calliope and REX facilities performed within the ASIF program using alanine-EPR dosimeters has provided critical insights into the beam distribution within the REX irradiation chamber. The results of the experimental campaign presented in this report are important for understanding the spatial homogeneity of the electron beam which is essential for ensuring uniform irradiation of samples. The consistency between the dose measurements from alanine dosimeters and from HD-V2 radiochromic films validates the calibration procedures employed and ensures the reliability of the dose estimates for electron irradiation at the REX facility.

The results from this study clearly show that the dose delivered by REX electron beam decreases with the distance from the linac due to beam spread in air. The transverse beam profile has a gaussian distribution maintaining approximately  $\pm 10\%$  homogeneity within a circular spot of about 32 mm to 43 mm in diameter at a distance from the linac exit of 30 and 40 cm, respectively. The measurements show a horizontal offset increasing with the distance from the linac exit up to 1 cm at 40 cm, that will be considered in the setup of samples irradiations.

## Acknowledgements

The authors would like to acknowledge the staff of the Calliope facility (ENEA NUC-IRAD-GAM) as well as the staff of ENEA NUC-TECFIS-ACP for their support and availability during the experiments. This work was supported by the Italian Space Agency (ASI) under ASIF program (ENEA-ASI Agreement No. 2021-39-HH.0).

## References

- [1] F. H. Attix, W. C. Roesch, and E. Tochilin, *Radiation Dosimetry*. Academic Press, 1968.
- [2] Italian Space Agency, "ASI Supported Irradiation Facilities: Accordi ASI-ENEA, ASI-INFN", [Online]. Available: <https://www.asi.it/tecnologia-ingegneria-micro-e-nanosatelliti/ingegneria/asif/>
- [3] J. Bashyal, "Beer-Lambert Law: Statement, Derivation, Applications, Limitations." [Online]. Available: <https://scienceinfo.com/beer-lambert-law-statement/>
- [4] "ISO/ASTM 51607:2013 - Practice for use of the alanine-EPR dosimetry system." 2013. [Online]. Available: <https://www.iso.org/standard/62955.html>
- [5] L.- Chemistry, "EPR - Theory." [Online]. Available: [https://chem.libretexts.org/Bookshelves/Physical\\_and\\_Theoretical\\_Chemistry\\_Textbook\\_Maps/Supplemental\\_Modules\\_\(Physical\\_and\\_Theoretical\\_Chemistry\)/Spectroscopy/Magnetic\\_Resonance\\_Spectroscopies/Electron\\_Paramagnetic\\_Resonance/EPR\\_-\\_Theory](https://chem.libretexts.org/Bookshelves/Physical_and_Theoretical_Chemistry_Textbook_Maps/Supplemental_Modules_(Physical_and_Theoretical_Chemistry)/Spectroscopy/Magnetic_Resonance_Spectroscopies/Electron_Paramagnetic_Resonance/EPR_-_Theory)
- [6] "Università politecnica delle Marche. La spettroscopia EPR." [Online]. Available: [https://www.univpm.it/Entra/Engine/RAServeFile.php/f/P002330/allegati\\_0Ains/Chill\(0910\)Dia04EPR.pdf](https://www.univpm.it/Entra/Engine/RAServeFile.php/f/P002330/allegati_0Ains/Chill(0910)Dia04EPR.pdf).
- [7] "The University of Texas at Austin. What is EPR?" [Online]. Available: [https://sites.cns.utexas.edu/epr\\_facility/what-epr](https://sites.cns.utexas.edu/epr_facility/what-epr)
- [8] "Aerial." [Online]. Available: <https://aerial-crt.com/en/home/>.
- [9] B. D'Orsi et al., "Optimization of paper characterization procedures for cultural heritage," *RT/2024/2/ENEA*. 2024.
- [10] Ashland, "Gafchromic HD-V2." [Online]. Available: <http://www.gafchromic.com/0Agafchromic-film/radiotherapy-films/HD-V2/index.asp>.
- [11] S. Baccaro, A. Cemmi, I. Di Sarcina, and G. Ferrara, "Gamma irradiation Calliope facility at ENEA-Casaccia Research Centre (Rome, Italy)," *RT/2019/4/ENEA*, 2019.
- [12] "ISO/ASTM 51026:2015 Practice for using the Fricke dosimetry system," 2015.
- [13] M. Vadrucci, P. Ferrari, F. Borgognoni, and L. Campani, "The REX irradiation facility and its applications," *Nucl. Instruments Methods Phys. Res. Sect. A Accel. Spectrometers, Detect. Assoc. Equip.*, vol. 930, pp. 126–131, Jun. 2019, doi: 10.1016/J.NIMA.2019.02.066.
- [14] G. Bazzano et al., "Electron beam qualification at ENEA Frascati particle accelerators laboratory," in *Proceedings of the 14th International Particle Accelerator Conference (IPAC'23), Venice, Italy, May 7-12, 2023*.

- [15] IBA, "PPC05 Plane Parallel Chamber." [Online]. Available: <https://www.iba-dosimetry.com/%0Aproduct/ppc05-plane-parallel-chamber>
- [16] P. Casolaro, L. Campajola, and F. Di Capua, "The physics of radiochromic process: one calibration equation for all film types," *J. Instrum.*, vol. 14, 2019, doi: 10.1088/1748-0221/14/08/P08006.

ENEA  
Servizio Promozione e Comunicazione  
[www.enea.it](http://www.enea.it)

Stampa: Laboratorio Tecnografico ENEA - C.R. Frascati  
febbraio 2025